Materials Physics and Mechanics. 2023;51(1): 19-32
Research article
http://dx.doi.org/10.18149/MPM.5112023_3

Submitted: September 15, 2022
Approved: December 7, 2022
Accepted: January 20, 2023

Effect of nickel incorporation on structural and optical properties of zinc oxide thin films deposited by RF/DC sputtering technique

Mohibul Khan, Md Shahbaz Alam, Sk. Faruque Ahmed✉

Nanoscience Laboratory, Department of Physics, Aliah University, IIA/27, Newtown, Kolkata -700160, India

*e-mail:fahmed.phys@aliah.ac.in

Abstract: Reactive co-sputtering technique has been used to fabricate pure zinc oxide and nickel doped zinc oxide thin films on glass substrate at room temperature 30º C. The actual target of this experimental work was to investigate the effect of nickel incorporation on structural and optical properties of nickel doped zinc oxide thin films. The deposited samples were characterized by using Energy-Dispersive Analysis X-ray, X-Ray Diffractometer, Atomic Force Microscope, Fourier Transform Infrared Spectroscopy and Ultraviolet-visible spectrophotometer to investigate the doping growth, structural crystallinity, surface morphology, chemical bonding information and optical properties. Scanning electron microscope has been used to measure the thickness of all deposited films. The X-Ray Diffractometer study of all deposited films reveals that the highly intensive peak has been found near glancing angle at 34.48° corresponds to miller indices (002), which confirmed the wurtzite hexagonal crystallite structure of zinc oxide that matched with JCPDS card no 36-1451. Crystallite size of deposited thin films is increased from 8 nm to 15 nm with the increasing of atomic % of nickel from 0 to 7.5 respectively in zinc oxide. The Fourier Transform Infrared Spectroscopy peak found at 432 cm^{-1} confirmed the deposited films are zinc oxide thin films. Optical band gap energy decreases from 3.15 eV to 2.21 eV where as the Urbach energy increases from 118meV to 243meVwith increasing of atomic % of nickel from 0 to 7.5 respectively.

Keywords: Ni-ZnO thin films; RF/DC sputtering technique; XRD; AFM; Optical Property; Urbach energy.

Acknowledgement. *The authors wish to acknowledge the University Grants Commission, New Delhi, India for the financial support under Maulana Azad National Fellowship (MANF) scheme during the execution of the work.*

Citation: Khan M., Alam M S, Ahmed S F. Effect of nickel incorporation on structural and optical properties of zinc oxide thin films deposited by RF/DC sputtering technique. *Materials Physics and Mechanics*. 2023;51(1): 19-32. DOI: 10.18149/MPM.5112023_3.

Introduction

Among all II–VI chalcogenide type semiconductors materials, nanocrystalline zinc oxide (whose direct wide band gap and exciton binding energy are 3.37 eV and 60 meV respectively) is one of the greatest acceptable interests for their environmentally safe and versatile application in the field of nanoscience and nanotechnology [1-3]. Past few decades, many researchers from different part of the world have been chosen zinc oxide (ZnO) materials for its multi–functional behaviors like as chemical stability, opto-electric, well luminescence property, good transparency, prominent electron mobility and piezoelectric properties [1-5]. Piezoelectric properties of ZnO thin films depend on its hexagonal crystalline structure [5]. Applications of ZnO thin films are most striking because of their low cost and

© M. Khan, Md.S.Alam, Sk.F. Ahmed, 2023.
Publisher: Peter the Great St. Petersburg Polytechnic University
This is an open access article under the CC BY-NC 4.0 license (https://creativecommons.org/li-censes/by-nc/4.0/)

also for the non-toxic behavior which is comparable with some oxides like CdO, In_2O_3 and SnO_2 [2,6]. Also, the low resistivity and high transmittance properties of ZnO have been found in the visible region [6]. This type of nano-range ZnO thin films has been used due to its extensively applications in optoelectronic devices [2,3,6]. Nowadays nano-range ZnO films are used in extensive area of science and technology like as UV protectors, solar cell, gas sensing devices, transparent FETs, antibacterial coatings, drug delivery devices, cancer treatment, transparent conducting oxides, photo catalysis, Schottky diodes, light emitting diodes, flat panel displays, spintronics, computer screen, high mobility transistor, laser diodes, surface acoustic devices, smart windows, smartphone display, varistors, high electron mobility, chemical sensors, photo voltaic cells and transparent electrodes [1-11]. The doping effect of different elements such as Au, Al, Sb, N, Ga, Cu, Mn, Ti, Ag, Co, Mo, In, Sn, Fe, and V with pure ZnO on physical, optical, electrical, and dielectric properties have been reported [1-16]. The position of metal element nickel (Ni) in the periodic table is 10th group of 4th period along with Fe and Co. This transition metal which gradually loses its strong metallic behavior is a very good conductor of electric and heat. Ni has three oxidation states which are +2, +3 and +4. Among all oxidation states +2 is the most significant state [17]. The electro negativity behavior of Ni suggests a suitable bonding attraction for with other elements. 0.69 Å is the ionic radii of Ni^{+2} which is familiar with Zn^{+2} (0.74 Å) [17]. The structure and valance of Ni and Zn elements are similar. This can be presumed that the hexagonal crystalline structure of ZnO is not changing if Ni^{+2} ion replaced by Zn^{+2} ion in pure ZnO lattice. The changing effect of Ni on different properties that i.e, physical, optical, electrical, and dielectric with ZnO have been reported earlier [17,18]. In this experimental work, the changes in structural and optical properties of ZnO thin film with Ni incorporation have been studied in detail.

Nickel doped ZnO (NZO) thin films are deposited by several physical and chemical techniques such as chemical bath deposition, photochemical deposition, cyclic voltammetry, sol-gel preparation, low temperature aqueous solution route, spray pyrolysis, metal organic chemical vapor deposition, Radio Frequency (RF) sputtering, screen printing, Direct Current (DC) sputtering, molecular beam epitaxy, DC and RF magnetron sputtering techniques [1-19]. In this scientific work, RF and DC co-reactive magnetron sputtering technique has been chosen to prepare pure ZnO and NZO thin films on glass substrate. This physical technique has been used due to its various advantageous properties like as low-temperature growth, good quality of nano-range thin films, large film area and controllable thickness of film [2,3].

In this current scientific research work, pure ZnO and NZO thin films deposited by reactive co sputtering technique where ZnO and Ni targets were used in RF shutter and DC shutter simultaneously. ZnO films have been doped with different atomic % of Ni for the better improvement of the structural and optical properties of the newly formed nano crystal thin films. Deposited nano-range pure ZnO and NZO films were characterized and analyzed by using X-Ray Diffractometer (XRD), Energy-Dispersive Analysis X-ray (EDAX), Fourier Transform Infrared Spectroscopy (FT-IR), Atomic Force Microscope (AFM), Scanning Electron Microscope (SEM) and Ultraviolet-visible (UV-VIS) Spectrophotometer. Optical characteristics as well as the optical band gap energy (E_g) measured from the transmittance spectra of the deposited films by using UV-VIS spectrophotometer. The change in optical transmittance, E_g and urbach energy (E_u) with different atomic % of Ni in the ZnO thin films has been explored in detail.

Experimental Details

Materials and deposition techniques. Pure ZnO and NZO nano-range films have been deposited for 30 min on commercial glass substrate by using DC/RF magnetron co-sputtering technique with the variation of atomic % of Ni from 0 to 7.5% respectively at room temperature 30°C. Source materials (ZnO and Ni targets) and commercial glass substrate of size 75 mm × 25 mm × 1.45 mm were purchased from Sigma-Aldrich Company. Purity, diameter, and thickness of both targets are 99.999%, 54 mm and 2 mm respectively. At 45 °C temperature, all substrates were ultrasonically cleaned by acetone and double distilled water separately and finally soaked with hot air gun.

Only ZnO target was used in RF gun and only Ni target was used in DC gun. Before making the film's deposition, Argon gas was used to clean the impurities of two targets by pre sputtering for 10 minutes. The Rotary pump and Turbo pump of the system has been used simultaneously to maintain the chamber pressure at 3.5×10^{-4} Pa. Argon (Ar) gas and Oxygen gas were used 15 sccm and 5 sccm respectively by mass flow controller (MFC) for deposition purpose. Argon gas has been used for its good sputtering behavior, whereas oxygen gas has been used to maintain oxygen rich growth during deposition. Oxygen gas is also important to reduce the intrinsic donor defects during deposition. The working pressure of the deposition chamber was maintained at 2.0 Pa. Three rotations per minute of all deposition substrates have been used to maintained uniform thickness and good surface morphology of films. Cathode shutters to substrate holder distance was kept at 70 mm for good quality of thin films deposition. During the deposition, RF power set at 100 watt which was fixed and DC voltage, which varies from 180 V to 240 V respectively. The atomic % of Ni varies from 2.6 to 7.5 with the variation of DC voltages from 180 V to 240 V respectively. Only RF power has been used in ZnO target for the formation of pure ZnO thin films. Details of deposition conditions are given below the Table 1.

Characterizations. The compositional, structural, morphological, chemical and optical properties of pure ZnO and NZO thin films have been investigated. The compositional property of pure ZnO and NZO thin films has been tested by EDAX (Oxford, model-7582). The crystallite structure of all deposited films has been investigated by using XRD (Bruker, D-8 Advance). Ambient based multimode AFM (Bruker, MultiMode-8) has been used to characterize the surface morphology of all deposited thin films. AFM measurements have been done in contact mode. A silicon probe has been used for scanning purpose which have a radius of curvature 10 nm, height 15 microns and standard chip size 1.6×1.6×0.4 mm. A cross sectional scanning electron microscope has been used to calculate the thickness of all deposited films. The FT-IR spectroscopy (IR Affinity-1S, Shimadzu, Japan) has been used to study the chemical bonding information of all deposited thin films. The optical characteristics of the deposited films have been study using a UV-Vis spectrophotometer (V-770, Jasco, Japan).

Table 1. Deposition conditions were maintained for the formation of crystallite thin films.

Parameters	Corresponding values
Base pressure / (Pa)	3.5×10^{-4}
Working pressure / (Pa)	2.0
Target	ZnO, Ni
Ar flow / (cm^3/min)	15
O_2 flow / (cm^3/min)	5
Deposition temperature / (°C)	30
Substrate rotate / (r/min)	3
RF power / (W)	100
DC voltage / (V)	180, 210, 240
Deposition time / (min)	30
Distance between target and substrate holder / (mm)	70

Results and discussions

Energy-Dispersive Analysis X-ray (EDAX) analysis. EDAX has been used to understand the doping growth of atomic % of Ni in ZnO nano-range thin film. The EDAX results of pure ZnO and 7.5 atomic % of Ni doped ZnO nano-range thin films are shown in Fig. 1(a, b). The confirmation of pure ZnO nano-range thin films has been confirmed by EDAX after finding sharp peak of Zinc (Zn) and Oxygen (O) in the thin film respectively, which shown in Fig 1(a). An additional peak of Ni has been found together with Zn and O peaks in the current deposited thin film, which confirmed the NZO nano-range thin film as shown in Fig. 1(b). Ni is a minor intense peak in the NZO nano-range thin film, whereas Zn and O is major intense peak. It has been identified that after incorporation of Ni in the NZO nano-range thin film decreased the atomic % of both Zn and O respectively.

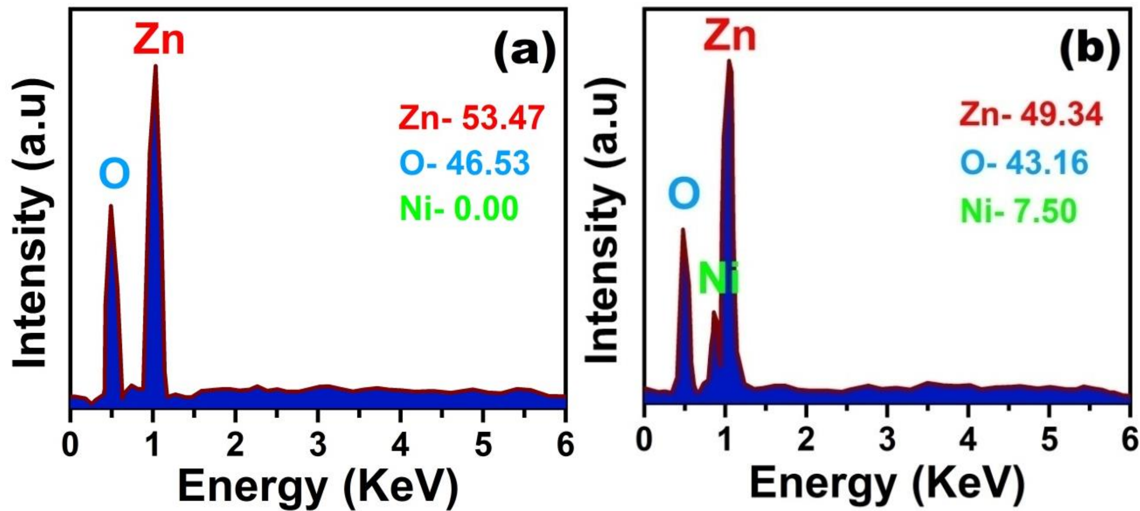

Fig. 1. EDAX spectra of NZO thin films: (a) 0.0 atomic % of Ni and (b) 7.5 atomic % Ni

X-Ray Diffractometer (XRD) study. The nature of structural crystalline property of pure ZnO and NZO films has been studied by XRD analysis. Cu-Kα radiation of wavelength λ = 1.5406 Å has been used to capture the XRD spectra of all deposited thin films in between 20° to 70° glancing angle. During the capturing of XRD spectra, the source voltage kept at 40 kV and source current kept at 40 mA. XRD patterns of deposited all films has been shown in Figs. 2 (a-d). The XRD pattern of all films has been recorded with the scan rate 2° per minute. Crystal structures of deposited thin films are two types like hexagonal wurtzite or cubic zinc blende which is depends on few deposition parameters [2,3]. The highly intensive peak has been found near glancing angle at 34.48° corresponds to miller indices (002), which confirmed the wurtzite hexagonal crystalline structure of ZnO that matched with JCPDS card no 36-1451 [2,3,16,18,20]. Peak intensity of deposited films increased slowly with the increasing of atomic % of Ni from 0 to 7.5 respectively. Debye-Scherrer formula has been used to calculate the crystallite sizes (D) of all films [2,3,21,22]

$$D^{-1} = \frac{\beta \, cos\theta}{K\lambda}, \quad (1)$$

where K (0.94), λ (1.5406 Å), β and θ are known as Scherer constant, wavelength of X-ray, full width of half maximum (FWHM) and Bragg's angle or glancing angle respectively.

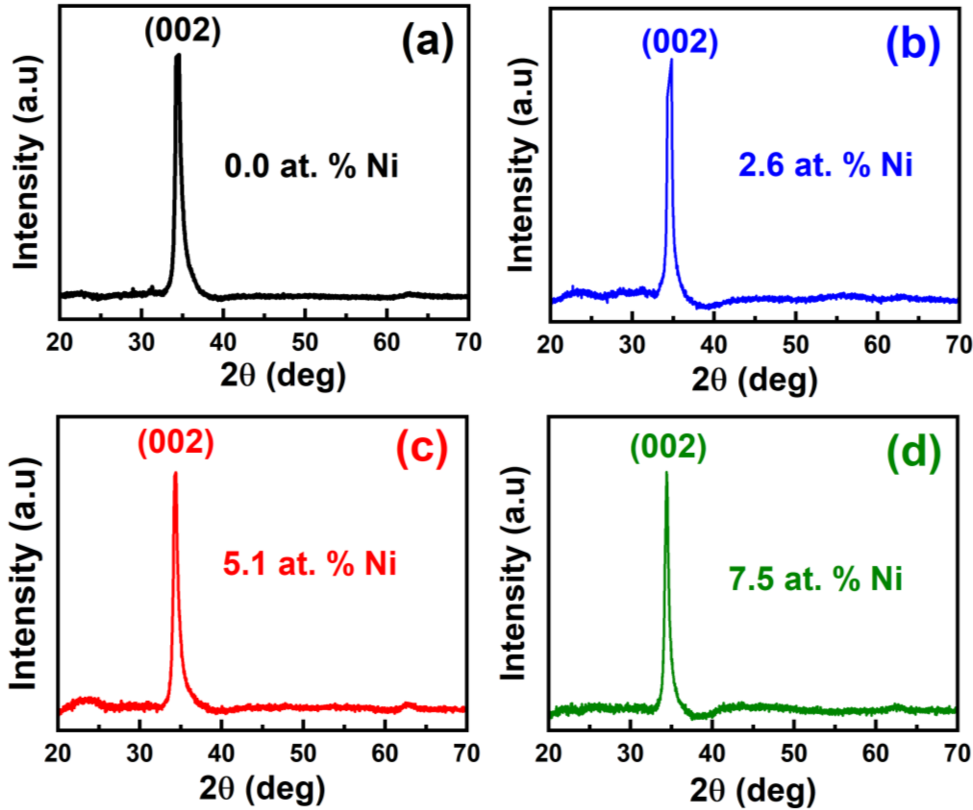

Fig. 2. (a-d). XRD patterns of NZO thin films deposited on glass substrates at different atomic % of Ni from;(a) Ni = 0, (b) Ni = 2.6, (c) Ni = 5.1, (d) Ni = 7.5% respectively

It is found that after increasing of atomic % of Ni from 0 to 7.5 the crystallite sizes of deposited films increased from 8 nm to 15 nm which are due to predominantly shifting of Ni^{2+} ion into the ZnO host lattice sites. As there is an inverse relation between crystallite size and FWHM, crystallites size increases from 8 nm to 15 nm where as β decreases from 1.06073° to 0.56425° respectively [22]. Equation 2 has been used to calculate the strain of all deposited films [20,22,23]

$$\varepsilon^{-1} = \frac{4}{(\beta cos\theta)} \quad . \tag{2}$$

After calculating the strain of all deposited films, it has been found that it is decreased from 44.18 × 10^{-4} to 23.5 × 10^{-4} with the increasing of atomic % of Ni from 0 to 7.5 respectively. Equation 3 is known as Bragg's equation, which has been used to calculate the interplanar spacing (d) of pure ZnO and NZO all films [8,23,24]

$$\frac{1}{d} = \frac{(2\,sin\theta)}{n\lambda}, \tag{3}$$

where n is diffraction order. Equation 4 has been used to calculate the lattice constants of deposited all films [8,24]

$$d^{-2} = \left[\frac{4}{3a^2}(h^2 + hk + k^2)\right] + \frac{l^2}{c^2}, \tag{4}$$

where (a,c) and (hkl) are lattice constant and miller indices. The lattice constant c slightly varies from 5.198 Å to 5.206 Å due to the substitution of Ni^{2+} ion instead of Zn^{2+} ion at their respective lattice sites. It was clearly observed that decrease in strain causes increased in crystallite size and increased in lattice constants [17,23].The values of glancing angles (2θ), Full Width Half Maxima (β), crystallite sizes (D), strain (ε), interplanar spacing (d) and lattice constant (c) are shown in Table 2.

Table2. XRD data of NZO thin films at different atomic % of Ni.

Atomic % of Ni	2θ (deg)	β (deg)	D (nm)	d (Å)	εX 10^{-4}	c (Å)
0.0	34.48	1.06073	8	2.599	44.18	5.198
2.6	34.46	0.86254	10	2.600	35.93	5.200
5.1	34.44	0.70253	12	2.602	29.26	5.204
7.5	34.42	0.56425	15	2.603	23.50	5.206

Atomic Force Microscope (AFM) study. Scanning probe AFM has been used to study the morphological property of deposited pure ZnO and NZO films surface. The surface image which has been captured by highly resolute AFM micrograph is homogeneous and uniform. Two-dimensional (2-D) AFM surface images of pure ZnO and NZO thin films and their corresponding histograms are shown in Fig. 3 (a-d). AFM images of all films display that the surface morphological characteristic varies with adding atomic % of Ni from 0 to 7.5 with pure ZnO respectively is shown in Fig. 3(a, b). The reflecting and scattering characteristic of transmitted light depend on the surface of morphological roughness of all deposited films. It has been found that the grain sizes of all films increases with increasing the roughness of the morphological surfaces, where the roughness of the morphological surfaces increases with adding atomic % of Ni from 0 to 7.5 with pure ZnO respectively. Histogram which is shown in Fig. 3 (c-d) exhibits that grain sizes of deposited films increased from 7 nm to 19 nm with adding atomic % of Ni from 0 to 7.5 with pure ZnO respectively. Grain size which has measured by AFM of ZnO film is lower than that calculated from XRD of same film. Grain size which has measured by AFM of NZO films is greater than the grain size calculated from XRD of same films. The bigger grain size which has been found in AFM of all films is caused by the agglomeration of lesser crystals, where XRD gives report about the mean grain size which coherently scatters the X-rays [25,26].

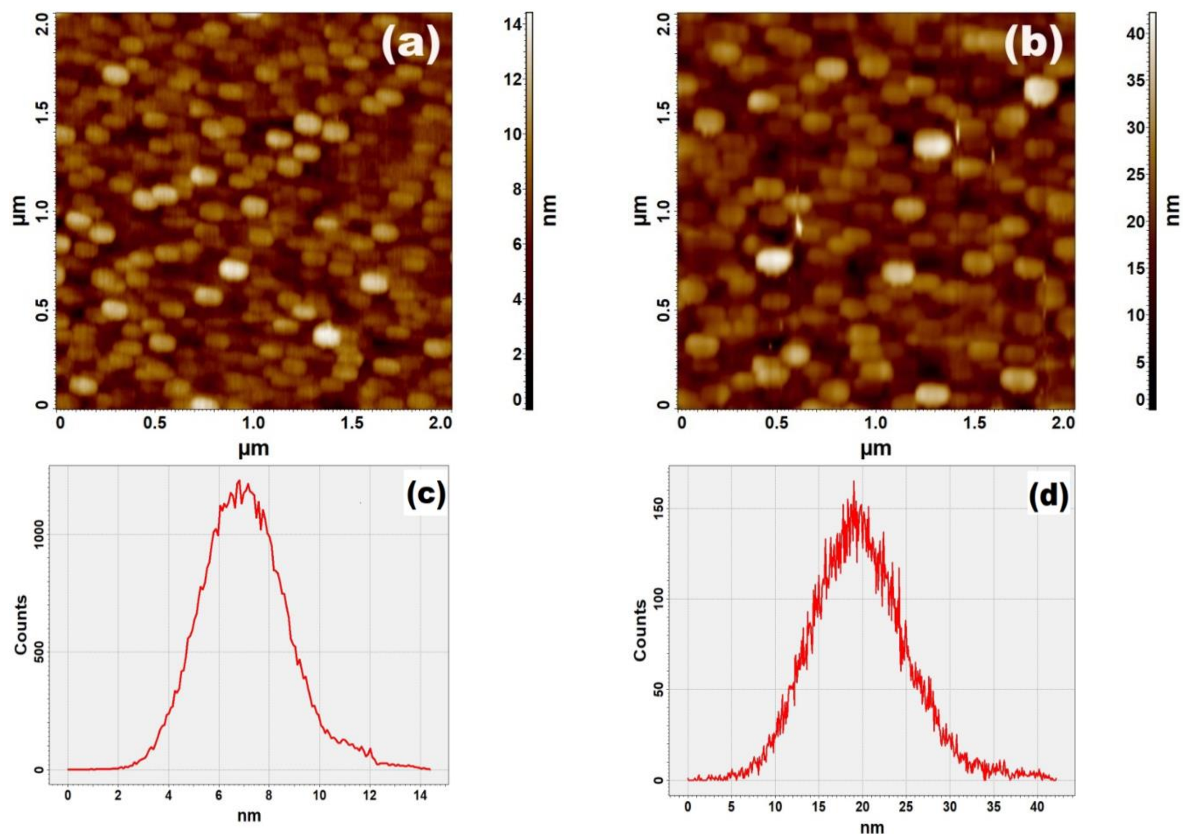

Fig. 3. Two-dimensional AFM images of NZO thin films: (a) 0.0 atomic % of Ni, (b) 7.5 atomic of Ni (c) and (d) the corresponding histogram

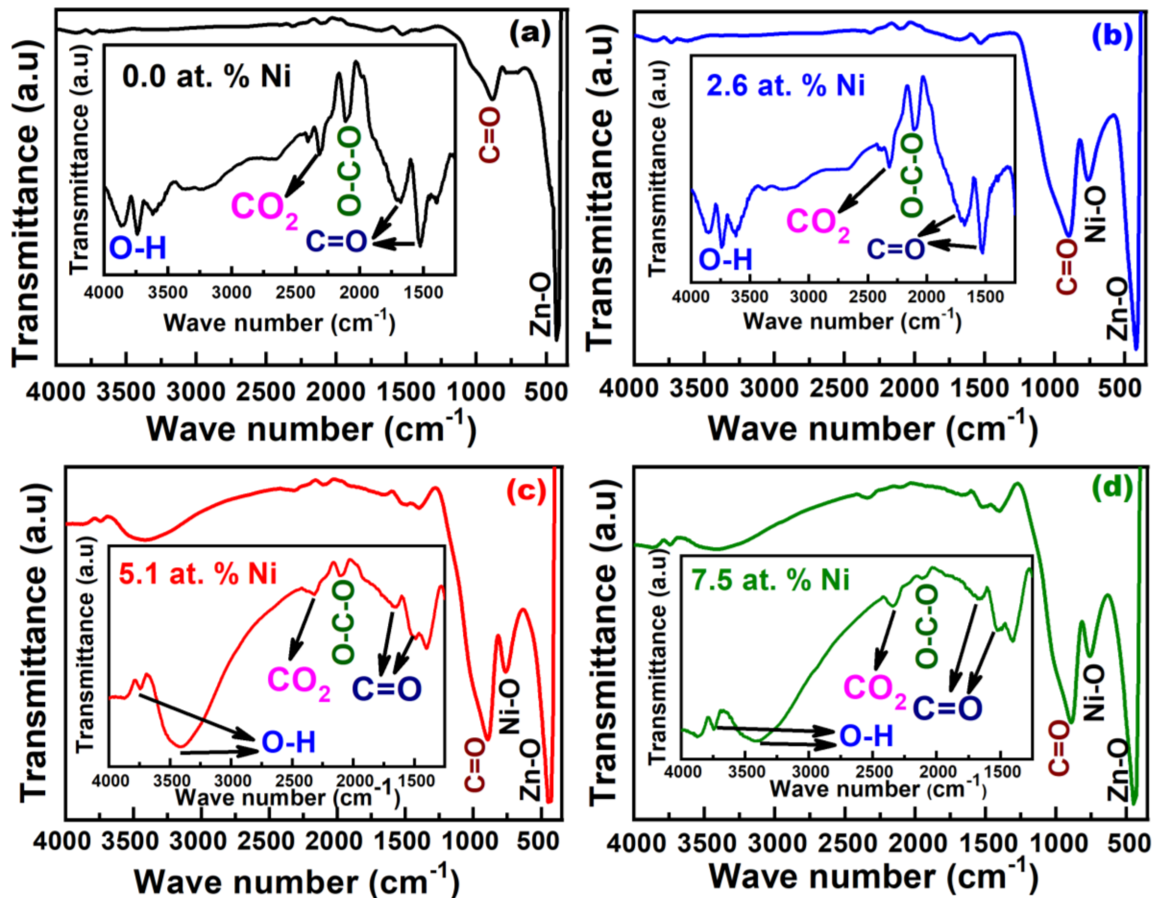

Fig. 4. (a-d) FT-IR spectra of NZO thin films with variation of atomic % of Ni from; (a) Ni = 0, (b) Ni = 2.6, (c) Ni = 5.1, (d) Ni = 7.5 respectively

Fourier Transform Infrared Spectroscopy (FT-IR) study. Chemical compositions of pure ZnO and NZO films have been observed by using FT-IR spectrum in 400 cm^{-1} to 4000 cm^{-1} the frequency at room temperature 30 $^{\circ}$C is shown in Fig. 4 (a-d). As all films deposited on glass substrate, so plane glass substrate has been used as reference for the measurement of FT-IR absorption spectra to eliminate the absorption peak. The structural and molecular arrangements of pure and Ni doped ZnO thin films on glass substrates have been examined by using FT-IR spectrum. The FT-IR frequency 400 cm^{-1} to 4000 cm^{-1} separated in two parts. The first part is 400 cm^{-1} to 1600 cm^{-1}. This part is known as fingerprint region and in this region stretching and bending vibrations are occurs. Whereas the second part is 1600 cm^{-1} to 4000 cm^{-1}, which part is known as functional group region and in this region only stretching vibration is occurs. The FT-IR peaks which are shown in Fig. 4 (a-d) have been found due to the stretching and bending vibration of atom and molecules or functional groups. The FT-IR peaks intensity does not fix, it is depends on different deposition materials. Due to the stretching vibration of Zn-O bond in all deposited films a peak has been identified at near 432 cm^{-1}, which confirmed the deposited films are ZnO thin films [18,19,24]. One peak has been identified except Fig. 4(a) closed to 720 cm^{-1} due to stretching vibration of Ni-O band [27]. The stretching absorption peak has been found in all deposited films at near 890 cm^{-1} assigned as C=O peak.Two absorption peaks have been found at near 1528 cm^{-1} and 1680 cm^{-1}, which were assigned due to symmetric strong C=O bond and asymmetric C=O bond respectively [2,3,27]. One FT-IR peak has been found near at 2060 cm^{-1} assigned to O-C-O bond, which decreased very slowly with the increase of atomic % of Ni from 2.6 to 7.5 respectively [18]. The absorption peak of CO_2 molecules has been identified at near 2310 cm^{-1}, which attributed due to the run time of deposition or atmosphere during the FT-IR

analysis [24]. The absorption peak of O-H band has been found between 3740 cm^{-1} to 3830 cm^{-1} and 3420 cm^{-1} to 3450 cm^{-1}, which assigned for atmosphere during the FT-IR analysis [28,29]. These FT-IR results of all deposited films state that Ni^{2+} ions successfully incorporated into pure ZnOlattice site and also confirmed the wurtzite crystalline nature of all films.

Optical band gap energystudy. UV-Visible spectrophotometer has been used to study the optical property of pure ZnO and NZO thin films in the wavelength between 300 nm to 800 nm at room temperature of 30 ºC are shown in Fig. 5. Optical property of deposited films depends on transmittance spectra. Highly transmittance films are important for good quality optical property. Transmittance spectra of deposited films depends on deposition conditions. In visible region deposited films are showed a transmittance nearly 85 % due to low scattering or absorption losses. Transmittance spectra of all deposited films gradually decreases with adding atomic % of Ni from 2.6 to 7.5 within pure ZnO are shown in Fig. 5 as well as it shifts towards from visible region to near UV region.Optical transmittance is related to film thickness. It is decreases with increasing of film thickness [30]. Thickness of the deposited films increased from 250 nm to 350 nm with increasing atomic % of Ni from 0 to 7.5 respectively.

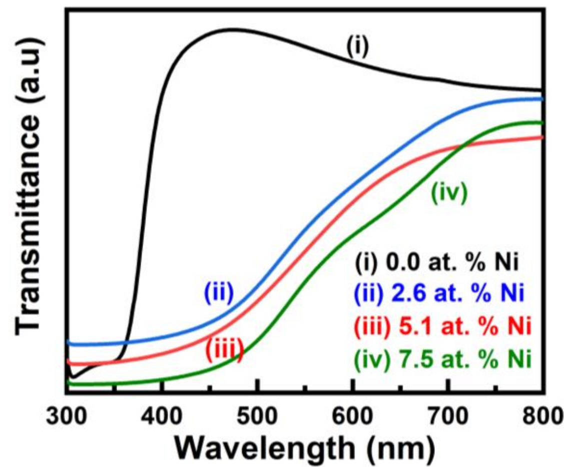

Fig. 5. Transmission spectra of NZO thin films with the variation of different atomic % of Ni from 0 to 7.5 respectively

The film thickness is calculated by using cross-sectional Scanning Electron Microscope images. Beer-Lambert law, which is getting from band theory of solid has been used to calculate the absorption coefficient (α) using the equation [8,22]

$$\alpha = \frac{1}{t}\ln\left(\frac{I_0}{I_t}\right), \quad (5)$$

where I_0, I_t and t are the intensity of incident light, intensity of transmitted light and thickness of deposited films respectively. The transmittance relation $T = \frac{I_t}{I_0}$ is known as the simplified form of Beer-Lambert formula. The energy of the optical band gap (E_g) of pure ZnO and NZO films has been calculated by using the Tauc expression [21,22,31]

$$(\alpha h\nu)^{1/m} = A(h\nu - E_g), \quad (6)$$

where A, $h\nu$ and m are constant, energy of the incident photon (h and ν are Planck's constant and frequency of the incident light respectively) and the different type of transition value. The value of m is different for different deposition semiconductor material. In this case the value of m is 1/2 as ZnO is directly allowed band gap materials [2,3,8]. In the case of directly allowed transition semiconductor material, the E_g of pure ZnO and NZO films has been

determined from the extrapolation of the straight line on the x-axis using $(\alpha h\upsilon)^2$ against $h\upsilon$ graph of different atomic % of Ni as shown in Fig. 6 (a-d). It is observed that the E_g of the deposited films decreases lightly with entering Ni into the ZnO layer. The obtained E_g of pure ZnO, ZnO: 2.6 at. % Ni, ZnO: 5.1 at. % Ni and ZnO: 7.5 at. % Ni films are 3.15, 2.59, 2.40 and 2.21 eV, respectively. It is observed that the E_g of pure and NZO films decreases due to increase in the grain size when atomic % of Ni increases [22]. The variation of E_g against different atomic % of Ni is shown in Fig. 7. It has been observed from Fig. 7 that the variation of the optical band gap energy of ZnO thin films is 0.94 eV (3.15 eV to 2.21 eV) by nickel doping which is better than other reported value such as 0.05 eV (3.33eV to 3.28eV), 0.08 eV (3.28eV to 3.20eV) and 0.51 eV (3.26 eV to 2.75 eV) respectively [32-34]. The potential advantage of NZO as an optical coating can be taken with controlling its optical band gap by changing the Ni content independently from other parameters.

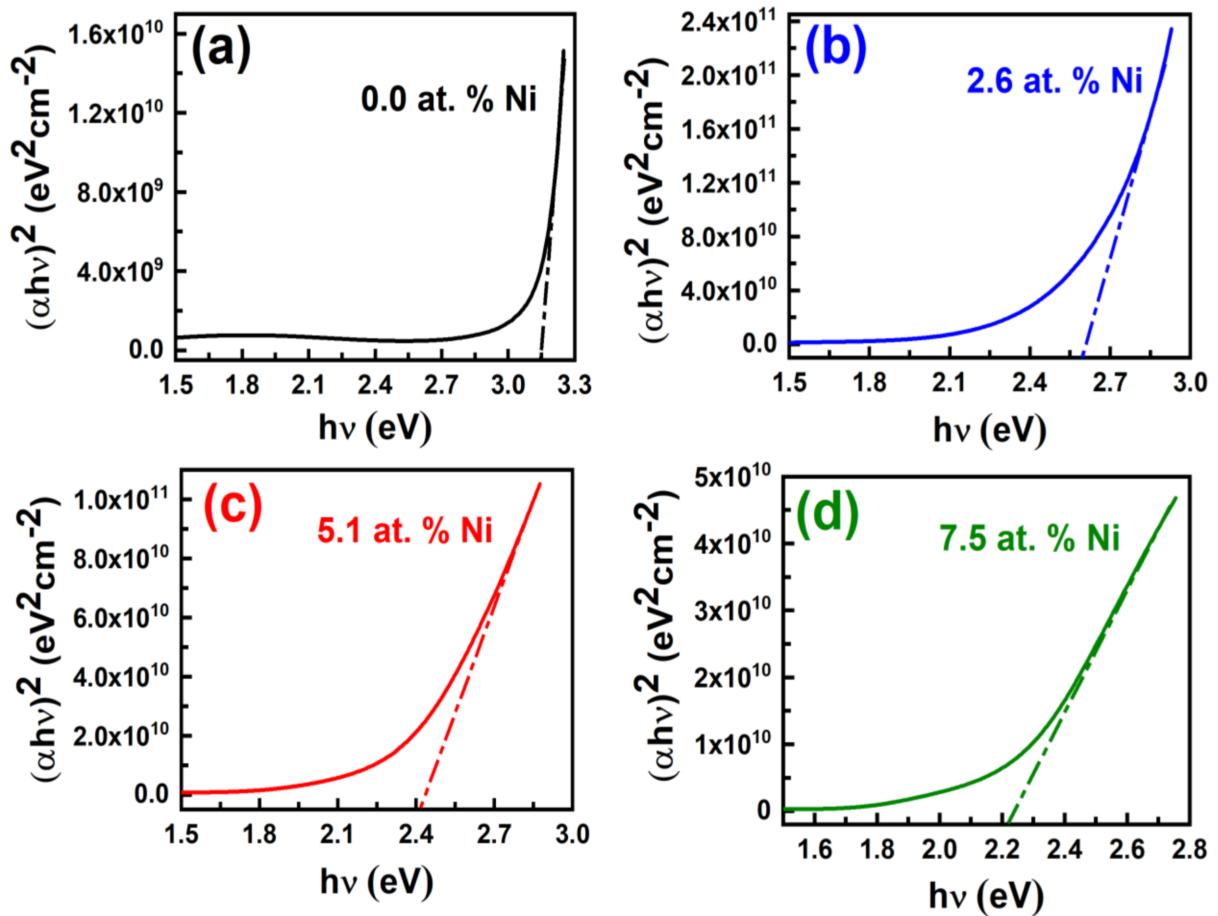

Fig. 6. (a-d) Tauc plot of $(\alpha h\nu)^2$ against hν at a different atomic % of Ni

Urbach energy. UV-vis spectrophotometers also been used to calculated Urbach energy (E_u) of deposited pure ZnO and NZO thin film. The E_u of deposited thin films has been found for the structural disorder of crystal, which is familiar as "band tail width" of localized energy states. The schematic band tail diagram of E_u of deposited films has been shown in Fig. 8(a). The diagrammatic expression of E_u of deposited crystalline film is shown by the formula

$$E_u = \Delta E_g - \Delta E_{g/} , \quad (7)$$

where ΔE_g and $\Delta E_{g/}$ are familiar as valence band to conduction band energy gap and valence band tail to conduction band tail energy gap respectively [3,22]. The E_u of deposited film is also familiar as disorder liness of phonon states or defect density. The E_u of deposited films is

calculated by usingan exponential function below the slope of absorption of band edge [35,36].

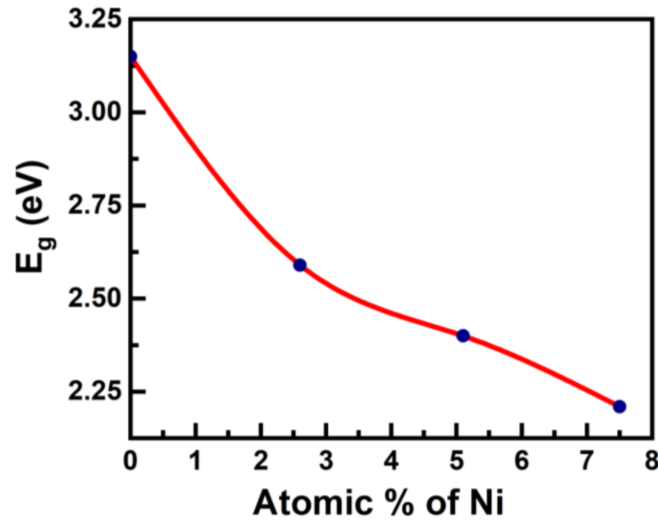

Fig. 7. Variation of E_g against different atomic % of Ni from 0 to 7.5 respectively

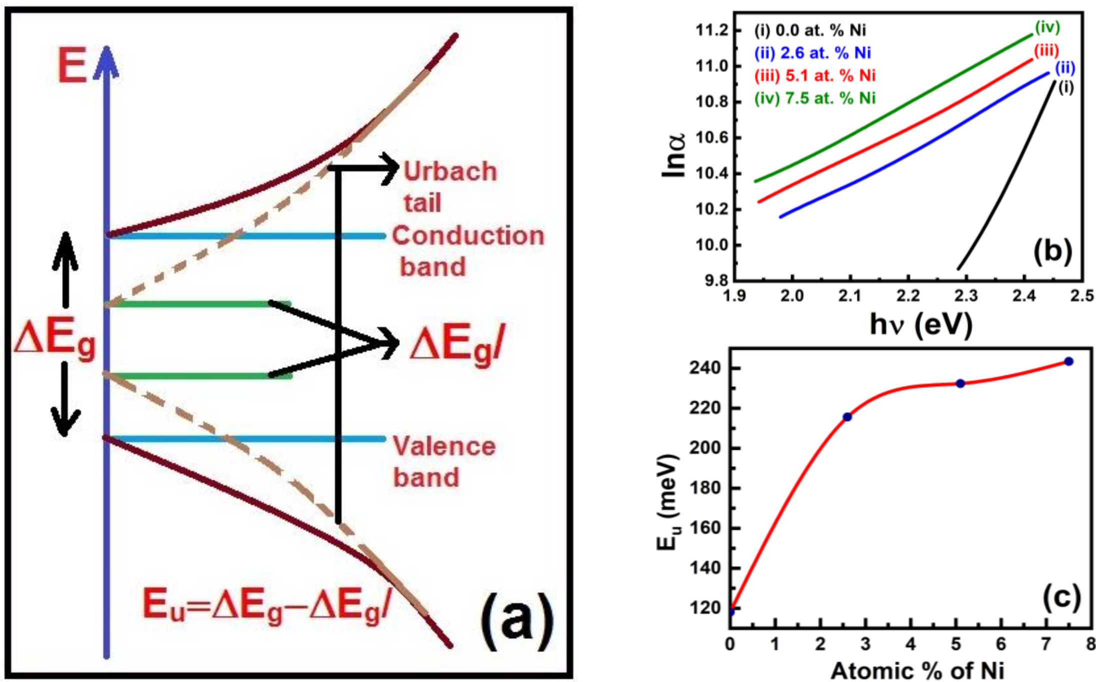

Fig. 8. (a) Schematic diagram of band tail of Urbach energy, (b) a plot of lnα vs. $h\nu$ of pure ZnO and NZO thin films with different at. % of Ni, (c) Variation of Urbach energy (E_u) of Ni doped ZnO thin films with atomic % of Ni

The absorption band edge of deposited films has been generated for the interaction of electron–phonon or exciting–phonon. Theoptical-electronic transitions of the compound which happened in between excited and near localized states is calculated from steepness parameter of absorption band edge. The band of the compound which bending slowly is depending on the reduction of optical band gap. In the phonon states,the disorder of pure ZnO and NZO films will be high if E_u is also higher. The band tail of urbach of deposited films has been expressed by the formula [37-39]

$$ln\alpha_0 = ln\alpha + {h\nu}/{E_u}, \quad (8)$$

where α_0, α and $h\nu$ are constant, absorption coefficient and photon energy of the incident ray of light respectively. Band tail of E_u of pure ZnO and NZO films has been determined using the lnα versus hνplot, which shown in Fig. 8 (b). Semiconductor Group (II-VI) chalcogenide materials urbach band tail depends on severalworkable defects which are structural disorder, interaction between carrier-impurity and carrier-phonon etc. [2,40]. In the phonon states of crystalline structure, the E_u of deposited films directly provides several efficient information about thermal disorderliness and the occupancy level [40].The exponential increasing of α of deposited pure ZnO and NZO films can be stated from the transitions of the density of states between valence to conduction band and also the shape and size of tails. The structural and thermal disorderliness of deposited films can be determined from Skettrup's theory, which modeled as an Einstein oscillator [40].

Generally, the E_g of deposited films is inversely related to E_u [40]. It is found that E_u of deposited films increases with increasing of atomic % of Ni from 0 to 7.5 respectively within pure ZnO. The graph between E_u versus atomic % of Ni shown in Fig. 8(c). The E_u of deposited films increases from 118 meV to 243 meV with the increasing of atomic % of Ni from 0 to 7.5 respectively within ZnO. The disorderliness of deposited pure ZnO and NZO films also increases with the increase of E_u. The slowly increasing state of E_u indicate that from tail to tail and band to tail transitions and redistribution of states severally [41]. Moreover it was found that the E_g of deposited films decrease due to the increase of the band tail of E_u [3,41].

Conclusions

In this experimental research work, pure ZnO and NZO thin films have been synthesized on the glass substrates via RF/DC reactive co-sputtering technique. XRD, AFM and FT-IR spectroscopy have been used to characterize the nanostructure crystallinity, surface morphology and chemical compositions of the pure ZnO and NZO thin films respectively. Crystallite sizes of deposited thin films which are measured by XRD are increased from 8 nm to 15 nm with the increasing of atomic % of Ni from 0 to 7.5 respectively in ZnO. Grain sizes of deposited films which are determined by AFM increased from 7 nm to 19 nm with adding atomic % of Ni from 0 to 7.5 with pure ZnO respectively. The FT-IR peaks which are found near 432 cm^{-1} and 755 cm^{-1} confirmed the deposited films are pure ZnO and NZO thin films. The E_g of pure and NZO thin films has been investigated by UV-Vis spectrophotometer which decreased from 3.15 eV to 2.21 eV with increasing the atomic % of Ni from 0 to 7.5 respectively at room temperature 30 °C. It is found that with increasing of atomic % of Ni from 0 to 7.5 the E_u increases from 118 meV to 243 meV respectively. The potential advantage of NZO as an optical coating can be taken with controlling its transparency and optical band gap by changing the Ni content independently of other parameters.

References

1. Sajjad M, Ullah I, Khan MI, Khan J, Khan MY, Qureshi MT. Structural and optical properties of pure and copper doped zinc oxide nanoparticles. *Results Phys.* 2018;9: 1301-1309.

2. Khan M, Ahmed SF. Effect of the distance between cathode and substrate on structural and optical properties of zinc oxide thin films deposited by rf sputtering technique. *Mater. Phys. Mech.* 2021;47(6): 872-884.

3. Khan M, Alam MS, Ahmed SF. Synthesis and Characterization of Copper Doped Zinc Oxide Thin Films Deposited by RF/DC Sputtering Technique. *J. Shanghai Jiao Tong Univ. (Sci.).* 2022.

4. Imran M, Ahmed R, Afzal N, Rafique M. Copper ion implantation effects in ZnO film

deposited on flexible polymer by DC magnetron sputtering. *Vacuum*. 2019;165: 72-80.
5. Maiti UN, Ghosh PK, Ahmed SF, Mitra MK, Chattopadhyay KK. Structural, optical and photoelectron spectroscopic studies of nano/micro ZnO: Cd rods synthesized via sol-gel route. *J. Sol-Gel Sci. Technol*. 2007;41: 87-92.
6. Saha B, Das NS, Chattopadhyay KK. Combined effect of oxygen deficient point defects and Ni doping in radio frequency magnetron sputtering deposited ZnO thin films. *Thin solid Films*. 2014;562: 37-42.
7. Pandey B, Ghosh S, Srivastava P, Kabiraj D, Shripati T, Lalla NP. Synthesis of nanodimensionalZnO and Ni-doped ZnO thin films by atom beam sputtering and study of their physical properties. *Physica E*. 2009;41(7): 1164-1168.
8. Yusof AS, Hassan Z, Zainal N. Fabrication and characterization of copper doped zinc oxide by using Co-sputtering technique. *Mater. Res. Bull.* 2018;97: 314-318.
9. Hafdallah A, Djefaflia F, Saidane N. Structural and Optical Properties of ZnO Thin Films Deposited by Pyrolysis Spray Method: Effect of Substrate Temperature. *Optics*. 2018;7(2): 68-73.
10. Mukherjee N, Ahmed SF, Chattopadhyay KK, Mondal A. Role of solute and solvent on the deposition of ZnO thin films. *Electrochimica Acta.* 2009;54(16): 4015-4024.
11. Dietl T,Ohno H. Diluted ferromagnetic semiconductors: Physics and spintronic structures. *Rev. Mod. Phys.* 2014;86(1): 187-251.
12. Caglar Y, Caglar M, Ilican S, Aksoy S, Yakuphanoglu F. Effect of channel thickness on the field effect mobility of ZnO-TFT fabricated by sol gel process. *J. Alloys Compd.* 2015;621: 189-193.
13. Al-Hardan NH, Abdullah MJ, Ahmad H, Aziz AA, Low LY. Investigation on UV photo detector behaviour of RF-sputtered ZnO by impedance spectroscopy. *Solid State Electron*. 2011;55(1): 59-63.
14. Khosravi P, KarimzadehF,Salimijazi HR, Abdi Y. Structural, optical and electrical properties of co-sputtered p-type ZnO: Cu thin-films. *Ceram. Int.* 2019;45(6): 7472-7479.
15. Kim H, Pique A, Horwitz JS, Murata H, Kafafi ZH, Gilmore CM, Chrisey DB. Effect of aluminum doping on zinc oxide thin films grown by pulsed laser deposition for organic light-emitting devices. *Thin Solid Films*. 2000;377-378: 798-802.
16. Zargar RA, KhanSUD, Khan MS, Arora M, Hafiz AK. Synthesis and Characterization of Screen Printed Zn0.97Cu0.03O Thick Film for Semiconductor Device Applications. *Phys. Res. Int.* 2014;2014: 464809.
17. Ali MY, Khan MKR, Karim AMMT, Rahman MM, Kamruzzaman M. Effect of Ni doping on structure, morphology and opto-transport properties of spray pyrolised ZnO nano-fiber. *Heliyon*. 2020;6(3): e03588.
18. Husain S, Rahman F, Ali Nasir, Alvi PA. Nickel Sub-lattice Effects on the Optical Properties of ZnONanocrystals. *J. Optoelectron. Engineer*. 2013;1: 28-32.
19. Fattah ZA. Synthesis and characterization of nickel doped zinc oxide nanoparticles by sol-gel method. *Int. J. Engineer. Sci. Res. Technol*. 2016;5: 418-429.
20. Muthukumaran S. Gopalakrishnan R. Structural, FTIR and photoluminescence studies of Cu doped ZnO nanopowders by co-precipitation method. *Opt. Mat.* 2012;34: 1946-1953.
21. Ghosh PK, Maiti UN, Ahmed SF, Chattopadhyay KK. Photoluminescence and field emission properties of ZnS:Mn nanoparticles synthesized by rf-magnetron sputtering technique. *Opt. Mater*. 2007;29(12): 1584-1590.
22. Khan M, Alam MS, Saha B, Ahmed SF. Synthesis and characterization of cadmium sulfide (CdS) thin films by cyclic voltammetry technique. *Mater. Today: Proceed*. 2021;47: 2351-2357.
23. Raja K, Ramesh PS, Geetha D. Synthesis, structural and optical properties of ZnO and Ni-doped ZnO hexagonal nanorods by Co-precipitation method. *Spectrochim. Acta. A Mol.*

*Biomol. Spectrosc.*2014;120: 19-24.
24. Elhamdi I, Souissi H, Taktak O, Elghoul J, Kammoun S, Dhahri E, Costa FO. Experimental and modeling study of ZnO:Ni nanoparticles for near-infrared light emitting diodes. *RSC Adv*. 2022;12: 13074-13086.
25. Abuelwafa AA, Denglawey AE, Dongol M, Nahass MME, Soga T. Influence of annealing temperature on structural and optical properties of nanocrystalline Platinum octaethylporphyrin (PtOEP) thin films. *Opt. Mater*. 2015;49: 271-278.
26. Ghosh PK, Maiti UN, Ahmed SF, Chattopadhyay KK.Highly conducting transparent nanocrystalline Cd1− xSnxS thin film synthesized by RF magnetron sputtering and studies on its optical, electrical and field emission properties. *Sol. Energy Mater. Sol. Cells*. 2006;90(16): 2616-2629.
27. Siddique MN, Ali T, Ahmed A, Tripathi P. Enhanced electrical and thermal properties of pure and Ni substituted ZnO Nanoparticles. *Nano-Struct. Nano-Objects*. 2018;16: 156-166.
28. Alamdari S, Ghamsari MS, Lee C, Han W, Park HH, Tafreshi MJ, Afarideh H, Ara MHM. Preparation and Characterization of Zinc Oxide Nanoparticles Using Leaf Extract of Sambucusebulus. *Appl. Sci*. 2020;10(10): 1-19.
29. Khan Z R, Khan M S, Zulfequar M, Khan M S. Optical and Structural Properties of ZnO Thin Films Fabricated by Sol-Gel Method. *Mater. Sci. App.* 2011;2: 340-345.
30. Shukla RK, Kumar N, Srivastava A. Pandey A. Pandey M. Optical and sensing properties of Al doped ZnO nanocrystalline thin films prepared by spray pyrolysis. *Mater Today: Proceed*. 2018;5(3): 9102- 9107.
31. Alam MS, Khan M, Ahmed SF. Nanostructure wrinkle thin films on flexible substrate: Tunable optical properties. *Mater. Today: Proceed*. 2022;49: 1401-1407.
32. Khalfallah B, Chaabouni F, AbaabM. Ni-doped ZnO films deposited by RF magnetron sputtering using raw powder target. *Indian. J. Physics*. 2019;93: 439–447.
33. Owoeye VA, Ajenifuja E, Adeoye EA, Osinkolu GA, Popoola AP. Microstructural and optical properties of Ni-doped ZnO thin films prepared by chemical spray pyrolysis technique. *Mater. Res. Express.* 2019;6(8): 086455.
34. Ma Z, Ren F, Deng Y, Volinsky AA. Structural, electrochemical and optical properties of Ni doped ZnO: Experimental and theoretical investigation. *Optik*. 2020;219: 165204.
35. Rai RC. Analysis of the Urbach tails in absorption spectra of undoped ZnO thin films. *J. Appl. Phys*. 2013;113(15): 153508.
36. Alam MS, Mukherjee N, Ahmed SF. Optical Properties of Diamond Like Carbon Nanocomposite Thin films. *AIP Conf. Proceed*. 2018;1953(1): 090018.
37. Ahmed SF, Banerjee D, Chattopadhyay KK. The influence of fluorine on the optical properties in diamond like carbon thin films. *Vacuum*.2010;84(6): 837-842.
38. Ahmed SF, Moon MW, Lee KR. Effect of silver doping on optical property of diamond like carbon films. *Thin Solid Films*.2009;517(14): 4035-4038.
39. Alam MS, Ghosh CK, Mukherjee N, Ahmed SF. Nanostructure evolution and optical properties of silver doped diamond like carbon thin film on soft polymer. *Adv.Sci.Lett.* 2018;24: 5731–5736.
40. Islam MA, Hossain MS, Aliyu MM, Chelvanathan P, Huda Q, Karim MR, Sopian K, Amin N. Comparison of Structural and Optical Properties of CdS Thin Films Grown by CSVT, CBD and Sputtering Techniques. *Energy Procedia*. 2013;33: 203-213.
41. Vettumperumal R, Kalyanaraman S, Santoshkumar B, Thangavel R. Estimation of electron–phonon coupling and Urbach energy in group-I elements doped ZnO nanoparticles and thin films by sol–gel method. *Mater. Res. Bull*. 2016;77: 101-110.

THE AUTHORS

Mohibul Khan
e-mail: khanmohibul2@gmail.com

Md Shahbaz Alam
e-mail: 786shahbaz92@gmail.com

Sk. Faruque Ahmed
e-mail: faruquekist@gmail.com